

Thermal conductivity of type-II superconductors in the mixed state: Electron-vortex scattering

Sergei Sergeenkov* and Marcel Ausloos

SUPRAS, Institute of Physics, University of Liege, B-4000, Liege, Belgium

(Received 25 January 1995)

Two types of electron scatterers, free (unpinned) vortices and pinned (via extended defects) vortices, are considered and their contribution to the electronic thermal magnetoconductivity of type-II superconductors is discussed. The theoretical predictions are found to be in reasonable agreement with some experimental data on the thermal conductivity of twinned and tweeded high- T_c superconductors in high magnetic fields.

I. INTRODUCTION

As is known,¹⁻⁴ fluxoids (quanta of applied magnetic field penetrating a type-II superconductor) can affect the thermal conductivity (TC) providing extra scattering mechanisms for phonons and electrons. In contrast to alloys (and "dirty" superconductors), where the phonon-fluxoid scattering dominates the observable TC, the case of "pure" type-II superconductors (including high- T_c superconductors⁵⁻⁸) suggests another possibility. For instance, in this case the conductivity is essentially due to electrons with mean free path much longer than the vortex core size. The BCS excitations outside the cores, apart from being scattered by impurities, will also be sensitive to the presence of nonsuperconducting (NS)-type boundaries between the superconducting matrix and the normal core of each fluxoid (as we shall see below, extended defects, as pinning centers for vortices, can essentially modify these NS boundaries). In general, the total TC κ consists of an electronic contribution κ_e limited by impurity scattering and a lattice contribution κ_{ph} limited by electron scattering. The first monotonically decreases with temperature due to the BCS pairing of electrons, while the second monotonically increases with T . As a result,⁴ at low temperatures ($T \ll T_c$), κ_{ph} dominates the Meissner state and region near B_{c1} , whereas at high temperatures ($T \geq T_c/2$), κ_e is the dominant contribution for all fields.

A very interesting study^{9,10} has been that of the TC in an applied magnetic field (up to 5 T) for twinned and untwinned single crystals of Y-Ba-Cu-O samples. It was shown that the behavior of $\kappa(B)$ departs from conventional superconductor models which predict a linear dependence for thermal magnetoresistivity (TMR)¹⁻⁴

$$\Delta W(T, B) \equiv W(T, B) - W(T, 0) = C_0(T)B, \quad (1)$$

assuming that the field just adds a term to $W(T, 0)$ depending on the number of vortices. In the Y-Ba-Cu-O samples examined in Refs. 9 and 10, such a behavior was found up to $B=1$ T, but markedly reduced thereafter. To fit the data, an unusual phenomenological form has been proposed for the observed TMR,^{9,10}

$$\Delta W_{\text{exp}}(T, B) = C(T)B \exp(-pB^q), \quad (2)$$

with $q = \frac{1}{4}$.

To clarify the role of extended defects in high-field thermal conductivity of high-temperature superconductors (HTS's), Bougrine *et al.*¹¹ have measured the TMR of twinned $\text{YBa}_2\text{Cu}_3\text{O}_7$ and tweeded $\text{YBa}_2(\text{Cu}_{0.95}\text{Fe}_{0.05})_3\text{O}_7$ crystals in applied magnetic field (up to 5 T). In accord with the interpolation formula suggested by Eq. (2), they found a hierarchy of the stretched exponential laws with q dependent on the type of the defect, namely, q was found to cross over with field from 1 to $\frac{1}{2}$ and from $\frac{1}{2}$ to $\frac{1}{4}$ for pure and iron-doped samples, respectively. Regarding a possible explanation for such an unexpected, defect-sensitive behavior of the observed TMR, we would like to point out that both conventional scattering mechanisms, that is, phonon-vortex and electron-vortex, result in the same linear law dependence (1) only (see, e.g., Refs. 1-4) and thus none of them can account for the observed stretched exponential behavior (2). At the same time, an exponential field dependence is known¹² to be a characteristic feature of the so-called vortex-limited proximity effect which is essentially electronic by its nature [since it is based on the local (near a defect) modulation of the superconducting order parameter], and which is proved to be quite active and significant in intrinsically defected (twinned) HTS crystals (see, e.g., Refs. 13 and 14). Besides, any reasonable scenario for the TMR of type-II superconductors in the mixed state should account for the pinning ability of the material under discussion. To take advantage of the above-mentioned dualism of extended defects (as pinning centers and as proximity-mediated structures at the same time) and to provide a plausible explanation of the unusual, stretched exponential high-field dependence of the observed TMR in intrinsically defected HTS crystals, in the present paper a modification of the conventional electron-vortex scattering mechanism is considered by taking into account the existence of two types of electron scatterers, free (unpinned) vortices and pinned (via extended defects) vortices.

II. ELECTRON-VORTEX SCATTERING

Since the electron mean free path is limited by scattering with fluxoids and electrons, we can write in terms of thermal magnetoresistivity and assume the collision processes independent,

$$\Delta W(T, B) \equiv W(T, B) - W(T, 0) = W_{ef}(T, B). \quad (3)$$

Here we made an assumption that the resistivity due to the impurity scattering, $W(T, 0)$, is field independent and hence all the field dependence of the observable TMR comes from the electron-vortex scattering, $W_{ef}(T, B)$. To get the explicit form of $W_{ef}(T, B)$, we assume that electrons are scattered by the vortex cores which behave as if they were cylinders of normal metal. The order of magnitude and the temperature and field dependence of the electron-vortex thermal conductivity can be deduced from the kinetic theory expression³

$$\kappa_{ef} \equiv W_{ef}^{-1} = \frac{1}{3} C_e v_F l_f, \quad (4)$$

where C_e is the electronic specific heat per unit volume, v_F the Fermi velocity, and $l_f(T, B)$ the electron mean free path due to the scattering of electrons by vortices.

A. Defect-free case

Let us consider first the case of electron scattering by unpinned vortices. In this case vortex-limited electron mean free path reads³

$$2\pi l_f(T, B) = a(B) \left[\frac{a(B)}{\xi(T)} \right], \quad (5)$$

where $a(B) = \sqrt{\phi_0/B}$ is the vortex lattice spacing, and (ξ/a) the probability that an electron intersects a vortex core of size $\xi(T)$ [$\xi(T) = \xi_0/\sqrt{1 - T^2/T_c^2}$ is the superconducting coherence length].

Inserting expression (5) into Eq. (4), we get for the TMR due to the scattering of electrons by unpinned vortices

$$W_{ef}(T, B) = W_n(T) \left[\frac{B}{B_{c2}^*} \right]. \quad (6)$$

Here $W_n(T) \equiv \kappa_{en}^{-1}(T)$, $\kappa_{en} = (\frac{1}{3})C_e v_F l_i$ is the electronic thermal conductivity in the normal state, l_i is the electron mean free path due to the impurity scattering, and $B_{c2}^* = \phi_0/2\pi\xi l_i$.

At this stage, it is interesting to point out that Eq. (6) strongly resembles the known expression for the so-called flux-flow resistivity in the mixed state of type-II superconductors,¹⁵ $\rho_{ff}(T, B) \approx \rho_n(T)(B/B_{c2})$, where ρ_n is the normal-state resistivity. In view of Eq. (6), we can write approximately $W_{ef}(T, B)/W_n \approx \rho_{ff}(T, B)/\rho_n$.

B. A single defect

The above-mentioned analogy between electrical and thermal resistivities suggests a way to describe the role of pinning in the mixed state electronic TMR. Indeed, according to the so-called thermal assisted flux-flow (TAFF) model,¹⁵ which is a natural generalization of the flux-flow regime, the existence of pinning [with a force density per unit vortex length $f_p(T, B)$] results in the following modification of the magnetoresistivity:

$$\rho_{\text{TAFF}}(T, B) \approx \rho_{ff}(T, B) \exp[-U(T, B)/k_B T], \quad (7)$$

where $U(T, B) \propto f_p(T, B)$ is the pinning energy. In terms of the thermal magnetoresistivity, the TAFF mechanism brings about the corresponding change of the electronic TMR due to electron scattering by pinned vortices,

$$W_{ef}^p(T, B) \approx W_{ef}(T, B) \exp[-U(T, B)/k_B T], \quad (8)$$

with $W_{ef}(T, B)$ given by Eq. (6). Thus, if our analogy is correct, the measurement of the thermal conductivity in applied magnetic field can provide interesting (and direct) information about the pinning characteristics of the material. If, however, we deal with the extended defects (such as dislocations, twin boundaries, etc.) as pinning centers for vortices, there exists another scattering mechanism which contributes to the observable TMR in intrinsically defected material. This mechanism is originated from the scattering of electrons by the vortices confined within a defect-mediated NS boundary. Indeed, the proximity-induced depletion of the superconducting order parameter near such a NS boundary will affect the probability of the electron scattering by pinned (via NS barrier) vortices and, in turn, results in the following change of the electron-vortex contribution to the observable TMR (cf. Ref. 12):

$$W_{ef}^d(T, B) = W_{ef}(T, B) \exp[-K_N(T, B)\delta], \quad (9)$$

where

$$K_N(T, B) = \frac{1}{\xi_N} \sqrt{1 + 6\beta\hbar/\pi\tau_{ef}}. \quad (10)$$

Here $\beta = 1/k_B T$, $K_N(T, B)$ is the inverse decaying length of the proximity coupling, δ and $\xi_N = \beta\hbar v_F/\pi$ are the thickness and coherence length of a normal metal, respectively, $W_{ef}(T, B)$ is given by Eq. (6), and \hbar/τ_{ef} is the depairing energy which in the vortex state of type-II superconductors reads¹ $\hbar/\tau_{ef}(T, B) = 2eBD_N$, where $D_N = v_F l_i/3$ is the diffusion coefficient. Notice a formal analogy between Eqs. (8) and (9). In fact, both of them describe the modification of the electron-vortex scattering in the presence of defects. At the same time, for the defect-free limit, when $\delta \rightarrow 0$, Eq. (9) coincides with the conventional expression (6).

Let us analyze the obtained results [Eqs. (9) and (10)]. At relatively small magnetic fields (so that $B \ll B_N$, where $B_N = \phi_0/4\pi l_i \xi_N$), we get in linear approximation

$$W_{ef}^d(T, B) \approx C_1(T) B \exp(-p_1 B), \quad B \ll B_N, \quad (11)$$

where $C_1(T) = c(T) \exp(-\delta/\xi_N)$, $c(T) = [W_n(T)/B_{c2}^*(T)]$, and $B^* \equiv 1/p_1 = \phi_0/2\pi l_i \delta$ is the so-called^{12, 14} proximity breakdown field.

At the same time, at large magnetic fields (when $B \gg B_N$), Eqs. (9) and (10) suggest the following behavior of the defect-mediated electron-vortex contribution to the TMR:

$$W_{ef}^d(T, B) \approx C_2(T) B \exp(-p_2 \sqrt{B}), \quad B \gg B_N \quad (12)$$

where $C_2(T) = c(T)$ and $p_2 = \sqrt{2\delta p_1/\xi_N}$. In Sec. III the above-obtained expressions (11) and (12) will be used to discuss some experimental data on thermal magnetoresistivity in defected high- T_c crystals.

C. Lattice of defects

Turning to a more realistic situation, let us consider now the case of electron scattering by a lattice of extended defects. To apply our scenario of proximity-mediated electron-vortex scattering for a multidefect situation, we assume that the electron scattering occurs in the normal regions distributed with an effective lattice spacing $a_{\text{eff}}(B)$ such that $a_{\text{eff}}^{-1}(B) = a^{-1}(B) + d^{-1}$, where $a(B)$ is the field-dependent vortex lattice spacing, and d the (field-independent) distance between extended defects. As a result, the thermal magnetoresistivity due to electron scattering by pinned vortices in the presence of the lattice of correlated defects reads [cf. Eq. (9)]

$$W_{\text{ef}}^l(T, B) = W_{\text{ef}}(T, B) \exp[-K_{\text{eff}}(T, B)\delta], \quad (13)$$

where

$$K_{\text{eff}}(T, B) = \frac{1}{\xi_N} \left\{ 1 + 4\pi \left[\frac{l_i}{a(B)} \right] \left[\frac{\xi_N}{a_{\text{eff}}(B)} \right] \right\}^{1/2}. \quad (14)$$

Notice that a single defect case considered in Sec. II B corresponds to the limit $d \rightarrow \infty$ when $a_{\text{eff}}(B)$ coincides with the vortex lattice spacing $a(B)$.

Depending on the relationship between two characteristic lattice parameters, $a(B)$ and d , there exist two distinctive regimes:

(i) $a(B) \ll d$; in this case there is no correlation between defects so that $a_{\text{eff}}(B) \simeq a(B)$ and the observable thermal magnetoresistivity will be dominated by a single defect electron-vortex scattering. Hence, in this limit $W_{\text{ef}}^l(T, B)$ reduces to the single defect TMR expression [see Eqs. (11) and (12)]. Figure 1(a) illustrates the field dependence ($B_0 = B_N$) of the normalized thermal magnetoconductivity $\kappa(B)/\kappa(0) \equiv W(T, 0)/W(T, B)$ calculated according to Eq. (13) with $d = 10a$ for different temperatures. As is seen, in this case thermal conductivity gradually decreases with applied field and the higher the temperature is, the less field dependent $\kappa(B)$ becomes.

(ii) $a(B) \gg d$; in this case $a_{\text{eff}}(B) \simeq d$ so that the density of defects is quite large and as a result the electron defect (rather than electron-vortex) scattering will dominate the observable TMR. The latter, in view of Eqs. (13) and (14), can be approximated for two field regions as follows:

$$W_{\text{ef}}^l(T, B) \simeq \begin{cases} C_3(T)B \exp(-p_3\sqrt{B}), & B \ll B_N^2/B_d \\ C_4(T)B \exp(-p_4B^{1/4}), & B \gg B_N^2/B_d \end{cases} \quad (15)$$

where $B_d = \phi_0/d^2$, $C_3(T) = C_1(T)$, $C_4(T) = C_2(T)$, $p_3 = p_1\sqrt{\phi_0/d^2}$, and $p_4 = p_2\sqrt{p_3/p_1}$. Figure 1(c) depicts the field behavior (with $B_0 = B_d$) of the normalized thermal magnetoconductivity $\kappa(B)/\kappa(0) \equiv W(T, 0)/W(T, B)$ given by Eq. (13) with $d = 0.1a$ for different temperatures. Notice that, in contrast with the previous case [Fig. 1(a)], the defect-dominated thermal conductivity shows some peculiarities in the applied magnetic field (similar to the ones observed in the mixed state of type-II superconductors¹⁻⁴). For example, with increasing field, $\kappa(B)$ first falls, then reaches a minimum (which shifts to lower fields and becomes more shallow with increasing temperature), and finally gradually increases towards the

normal-state value. For completeness, the intermediate case, when $d = a$, is shown in Fig. 1(b).

III. DISCUSSION

To compare the above model predictions with some experimental data, in Fig. 2 we present the log-log plot of the reduced excess TMR, $-\ln[\Delta W(T, B)/cB]$, versus applied magnetic field observed by Bougrine *et al.*¹¹ on the twinned $\text{YBa}_2\text{Cu}_3\text{O}_7$ (a) and tweeded

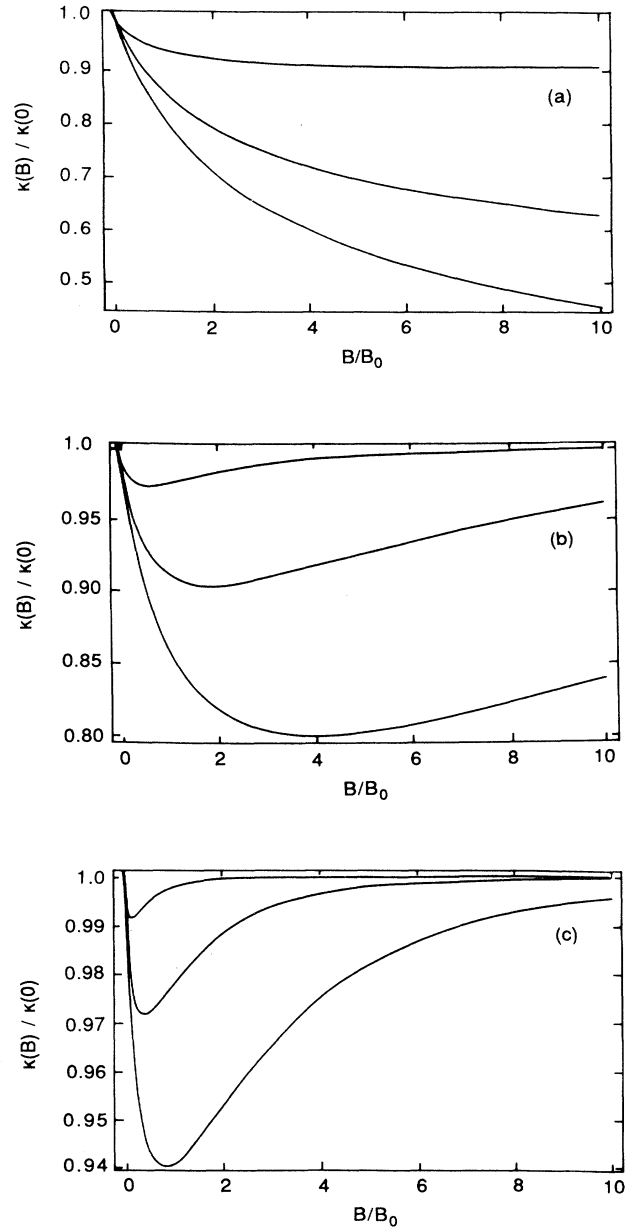


FIG. 1. Field-dependence of the normalized thermal conductivity, $\kappa(B)/\kappa(0)$, for three distinctive regions (see text): (a) $d = 10a$, (b) $d = a$, and (c) $d = 0.1a$. The curves, calculated according to Eq. (13), correspond to the following temperature (up to down): $T/T_c = 0.9, 0.7, \text{ and } 0.5$.

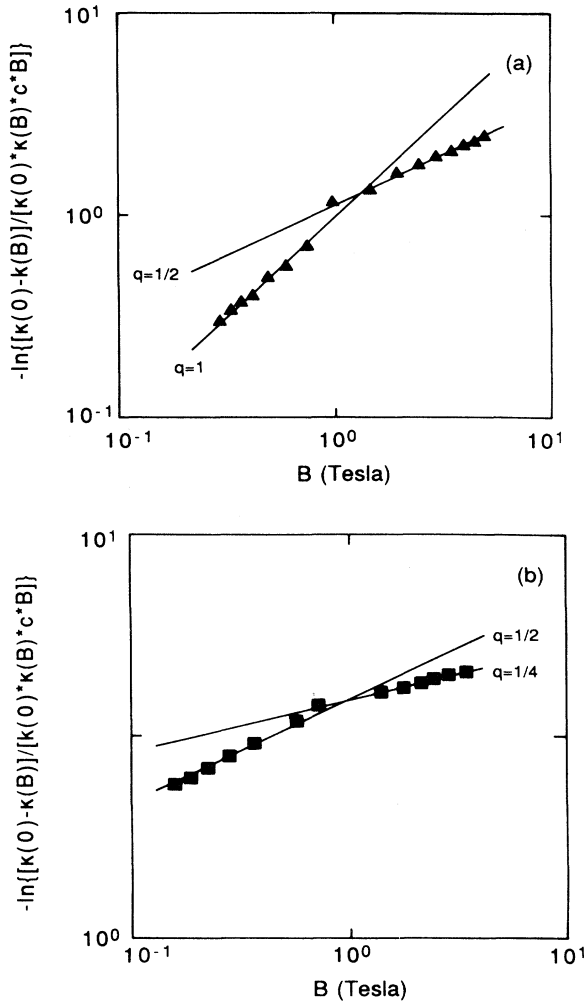


FIG. 2. The high-field data on reduced excess thermal magnetoresistivity of twinned $\text{YBa}_2\text{Cu}_3\text{O}_7$ (a) and tweeded $\text{YBa}_2(\text{Cu}_{0.95}\text{Fe}_{0.05})_3\text{O}_7$ (b) from Ref. 11 along with the best fits (solid lines) according to Eqs. (11), (12), and (15).

$\text{YBa}_2(\text{Cu}_{0.95}\text{Fe}_{0.05})_3\text{O}_7$ (b) crystals. The solid lines reproduce the best fit according to the asymptotic expressions (11), (12), and (15). To justify the applicability of the model equations to the description of the above experimental data, we propose the following scenario.

According to the measurements,¹⁶ the twin structure was found to be enhanced and replaced by finer tweed structure upon 5% Fe doping. Furthermore, as the high-resolution electron microscopy studies revealed,¹⁷ the mean intertwin distance d and twin-boundary thickness δ in pure Y-Ba-Cu-O are $d=200$ nm and $\delta=1-2$ nm, respectively. These should be compared with the inter-tweed distance $d=20$ nm and tweed-boundary (dislocation core) thickness $\delta=2-3$ nm for iron-doped Y-Ba-Cu-O.

Let us consider first the case of pure Y-Ba-Cu-O. When the applied field exceeds 1 T, vortex lattice parameter $a(B)$ becomes smaller than the interdefect spacing d , that is $a_{\text{eff}}(B) \simeq a(B)$; hence the electron scattering by uncorrelated pinned vortices starts to dominate the behavior of $W(B)$ [see Eqs. (11) and (12) and Fig. 2(a)].

Turning to the iron-doped case, we notice that up to the highest magnetic fields used in the experiments by Bougrine *et al.*,¹¹ the opposite situation takes place, namely, $d \ll a(B)$, leading to $a_{\text{eff}}(B) \simeq d$. Thus, in this case the electron defect scattering will dominate the observed $W(B)$ for all fields and the corresponding model expressions (for two distinctive crossover regimes) are provided by Eq. (15) [see Fig. 2(b)].

According to Eqs. (11) and (12), it follows from Fig. 2(a) that for pure Y-Ba-Cu-O, crossover (from $q=1$ to $q=\frac{1}{2}$) occurs at $B_{\text{cr}}^p = B_N \simeq 1$ T. Taking into account that for Y-Ba-Cu-O $v_F \simeq 2 \times 10^5$ m/s and thus $\xi_N(T=40 \text{ K}) \simeq 10$ nm, the above crossover field predicts $l_i^p = \phi_0 / 4\pi\xi_N B_{\text{cr}}^p \simeq 16$ nm for the electron mean free path in pure Y-Ba-Cu-O, in a reasonable agreement with the observations.⁵ Furthermore, taking the above l_i^p and using $\delta=2$ nm for a twin boundary thickness,¹⁷ we get an estimate for the breakdown field $B^* = \phi_0 / 2\pi l_i^p \delta \simeq 10$ T, which is quite comparable to the value deduced from the critical current measurements in pure Y-Ba-Cu-O. In a similar way, Fig. 2(b) along with Eq. (15) suggest that for Fe-doped Y-Ba-Cu-O crossover (from $q=\frac{1}{2}$ to $q=\frac{1}{4}$) takes place at $B_{\text{cr}}^d = B_N^2 / B_d \simeq 1$ T. Using $d=20$ nm (which corresponds to $B_d \simeq 5$ T) for the intertweed distance,¹⁷ the above equation provides an estimate of the electron mean free path, $l_i^d = \phi_0 / 4\pi\xi_N \sqrt{B_d B_{\text{cr}}^d}$, in Fe-doped Y-Ba-Cu-O. The result is $l_i^d / l_i^p \simeq 0.5$. To provide a more detailed verification of the model predictions, more experimental data on the thermal magnetoconductivity of superconductors with different (but well-controlled) defect structure are required.

In summary, incorporating two types of electron scatterers, free (unpinned) vortices and pinned (by the extended defects) vortices, into the conventional picture of the electron-vortex scattering mechanism, the electronic contribution to the thermal conductivity of type-II superconductors was discussed. The model predictions were compared with some experimental data on the thermal conductivity of twinned and tweeded high- T_c superconductors in high magnetic fields.

ACKNOWLEDGMENTS

Part of this work has been financially supported through the Impulse Program on High-Temperature Superconductors of Belgium Federal Services for Scientific, Technological, and Cultural (SSTC) Affairs under Contract No. SU/02/013.

*Permanent address: Frank Laboratory of Neutron Physics,
Joint Institute for Nuclear Research, 141980 Dubna, Moscow
region, Russia.

- ¹K. Maki, *Phys. Rev.* **158**, 397 (1967).
²J. Lowell and J. B. Sousa, *Phys. Lett.* **25A**, 469 (1967).
³J. B. Sousa, *Physica (Utrecht)* **55**, 507 (1971).
⁴W. F. Vinen *et al.*, *Physica (Utrecht)* **55**, 94 (1971).
⁵C. Uher, *J. Supercond.* **3**, 337 (1990).
⁶S. D. Peacor *et al.*, *Phys. Rev. B* **43**, 8721 (1991).
⁷Daming Zhu *et al.*, *Phys. Rev. B* **41**, 6605 (1990).
⁸V. Calzona *et al.*, *Europhys. Lett.* **13**, 181 (1990).
⁹R. A. Richardson *et al.*, *Phys. Rev. Lett.* **67**, 3856 (1991).
¹⁰A. V. Inyushkin *et al.*, *J. Supercond.* **7**, 331 (1994).
¹¹H. Bougrine *et al.*, *Solid State Commun.* **86**, 513 (1993).
¹²T. Y. Hsiang and D. K. Finnemore, *Phys. Rev. B* **22**, 154
(1980).
¹³G. Deutscher and K. A. Muller, *Phys. Rev. Lett.* **59**, 1745
(1987).
¹⁴P. England, *et al.*, *Appl. Phys. Lett.* **53**, 2336 (1988).
¹⁵P. H. Kes *et al.*, *Supercond. Sci. Technol.* **1**, 242 (1989).
¹⁶T. Krekels *et al.*, *Physica C* **173**, 361 (1991).
¹⁷Zhi-Xiong Cai *et al.*, *Philos. Mag. A* **65**, 921 (1992).